

Supplementary Figures and Figure Legends

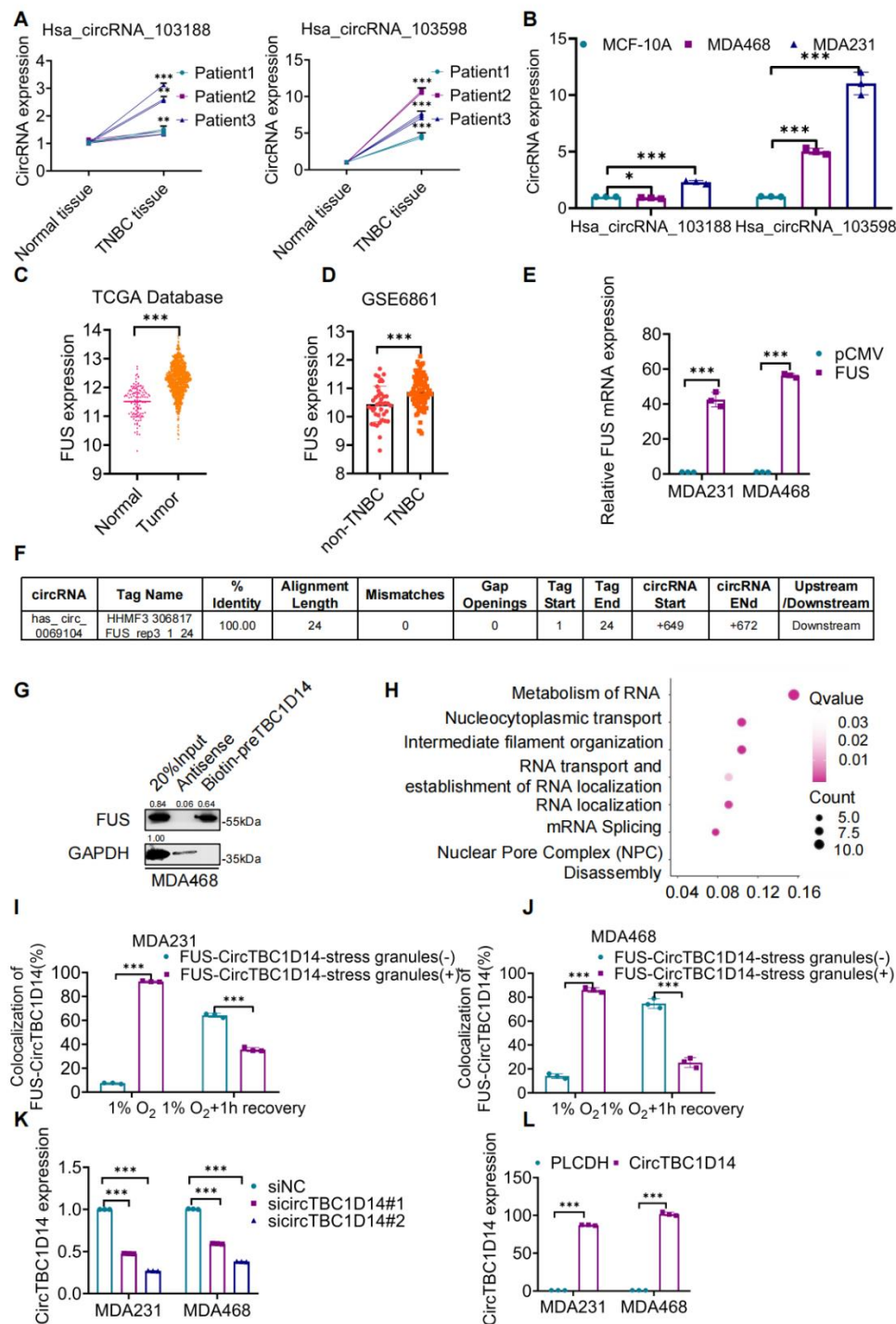


Figure. S1

**Figure. S1 FUS was an important regulator of circTBC1D14.** A) Quantitative real-time PCR analysis of has\_circRNA\_103188 and has\_circRNA\_103598 in breast cancer patient samples. Two-tailed unpaired t-test. B) Quantitative real-time PCR analysis of has\_circRNA\_103188 and

has\_circRNA\_103598 in MCF-10A, MDA468, and MDA231 cells. Two-tailed unpaired t-test. C) FUS expression analysis in TCGA database. Two-tailed unpaired t-test. D) FUS expression analysis in the GEO database. Two-tailed unpaired t-test. E) Quantitative real-time PCR analysis of FUS in MDA468 or MDA231 cells with FUS overexpression. Two-tailed unpaired t-test. F) Prediction of the flanking intron downstream of circTBC1D14 binding regions of FUS from online database Circular RNA Interactome. G) Western blot of RNA pull-down assays. H) GO analysis of RNA pulldown mass spectrometry and the related signaling pathways. I and J) Statistical diagram of colocalization percentage of FUS-CircTBC1D14 stress granules in MDA468 and MDA231 cells. Two-tailed unpaired t-test. K and L) Quantitative real-time PCR analysis of circTBC1D14 in MDA468 or MDA231 cells with circTBC1D14 overexpression or knockdown. Two-tailed unpaired t-test. The data are shown as the mean  $\pm$ SD, NS (no significance) \* $P < 0.05$  \*\* $P < 0.01$ , \*\*\* $P < 0.001$ .

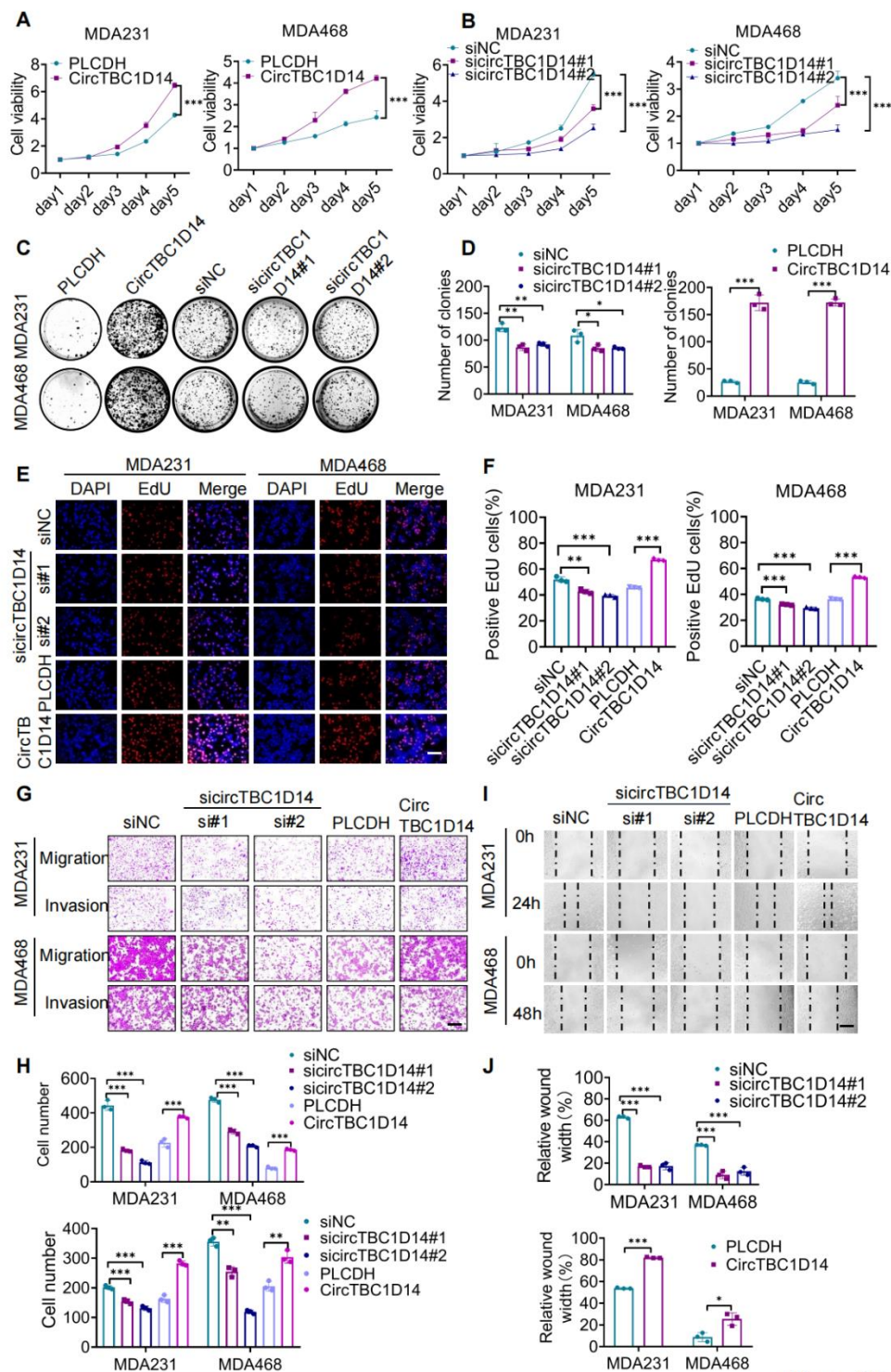


Figure. S2

**Figure. S2 CircTBC1D14 was essential for tumor progression and metastasis.** A and B) Cell viability of MDA231 and MDA468 cells with circTBC1D14 overexpression or knockdown compared to control cells. Two-tailed unpaired t-test. C) Clone formation of MDA231 and MDA468 cells with circTBC1D14 overexpression or knockdown compared to control cells. D)

Statistical diagram of C). Two-tailed unpaired t-test. E) EdU assay of MDA231 and MDA468 cells with circTBC1D14 overexpression or knockdown compared to control cells. Scale bar, 20  $\mu$ m. F) Statistical diagram of E). Two-tailed unpaired t-test. G) Transwell assay of MDA231 and MDA468 cells with circTBC1D14 overexpression or knockdown compared to control cells. Scale bar, 20  $\mu$ m. H) Statistical diagram of G). Two-tailed unpaired t-test. I) Wound healing assay of MDA231 and MDA468 cells with circTBC1D14 overexpression or knockdown compared to control cells. Scale bar, 20  $\mu$ m. J) Statistical diagram of I). Two-tailed unpaired t-test. The data are shown as the mean  $\pm$ SD, NS (no significance) \* $P$  < 0.05 \*\* $P$  < 0.01, \*\*\* $P$  < 0.001.

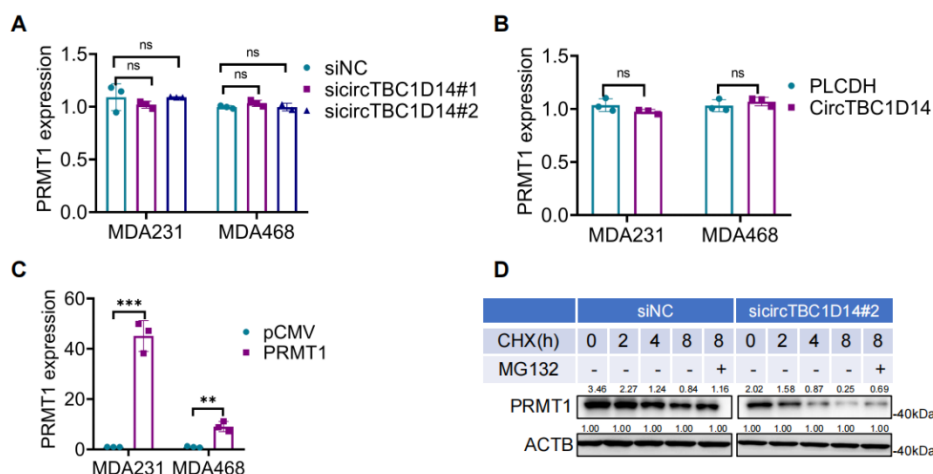


Figure. S3

**Figure. S3 Hypoxia-induced interaction between circTBC1D14 and PRMT1.** A and B) Quantitative real-time PCR analysis of PRMT1 expression in MDA468 or MDA231 cells with circTBC1D14 overexpression or knockdown. Two-tailed unpaired t-test. C) Quantitative real-time PCR analysis of RNA expression in MDA468 or MDA231 cells with PRMT1 overexpression. Two-tailed unpaired t-test. D) Western blot of PRMT1 with MG132 treatments pre-treated with CHX in time gradient. The data are shown as the mean  $\pm$ SD, NS (no significance) \* $P$  < 0.05 \*\* $P$  < 0.01, \*\*\* $P$  < 0.001.

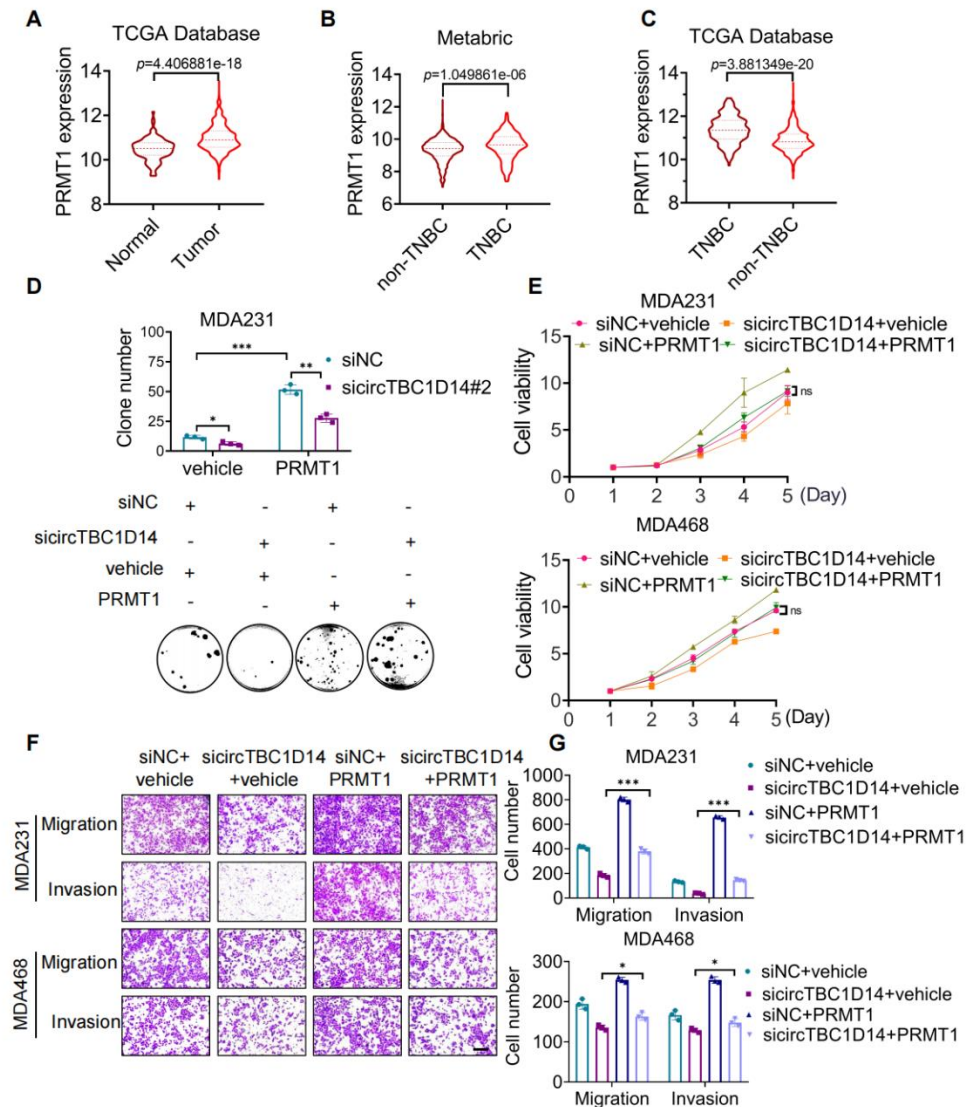


Figure. S4

**Figure. S4 CircTBC1D14 promoted tumor growth and metastasis by regulating PRMT1 in TNBC.** A and C) PRMT1 expression analysis in TCGA database. Two-tailed unpaired t-test. B)

PRMT1 expression analysis in Metabric database. Two-tailed unpaired t-test. D) Clone formation of circTBC1D14 knockdown in MDA231 cells with PRMT1 overexpressed. A statistic diagram was shown in the upper region. Two-tailed unpaired t-test. E) Cell viability of circTBC1D14 knockdown in MDA231 and MDA468 cells with PRMT1 overexpressed. Two-tailed unpaired t-test. F) Transwell of circTBC1D14 knockdown in MDA231 and MDA468 cells with PRMT1 overexpressed. G) Statistical diagram of F). Scale bar, 20  $\mu$ m. Two-tailed unpaired t-test. The data are shown as the mean  $\pm$ SD, NS (no significance) \* $P < 0.05$  \*\* $P < 0.01$ , \*\*\* $P < 0.001$ .



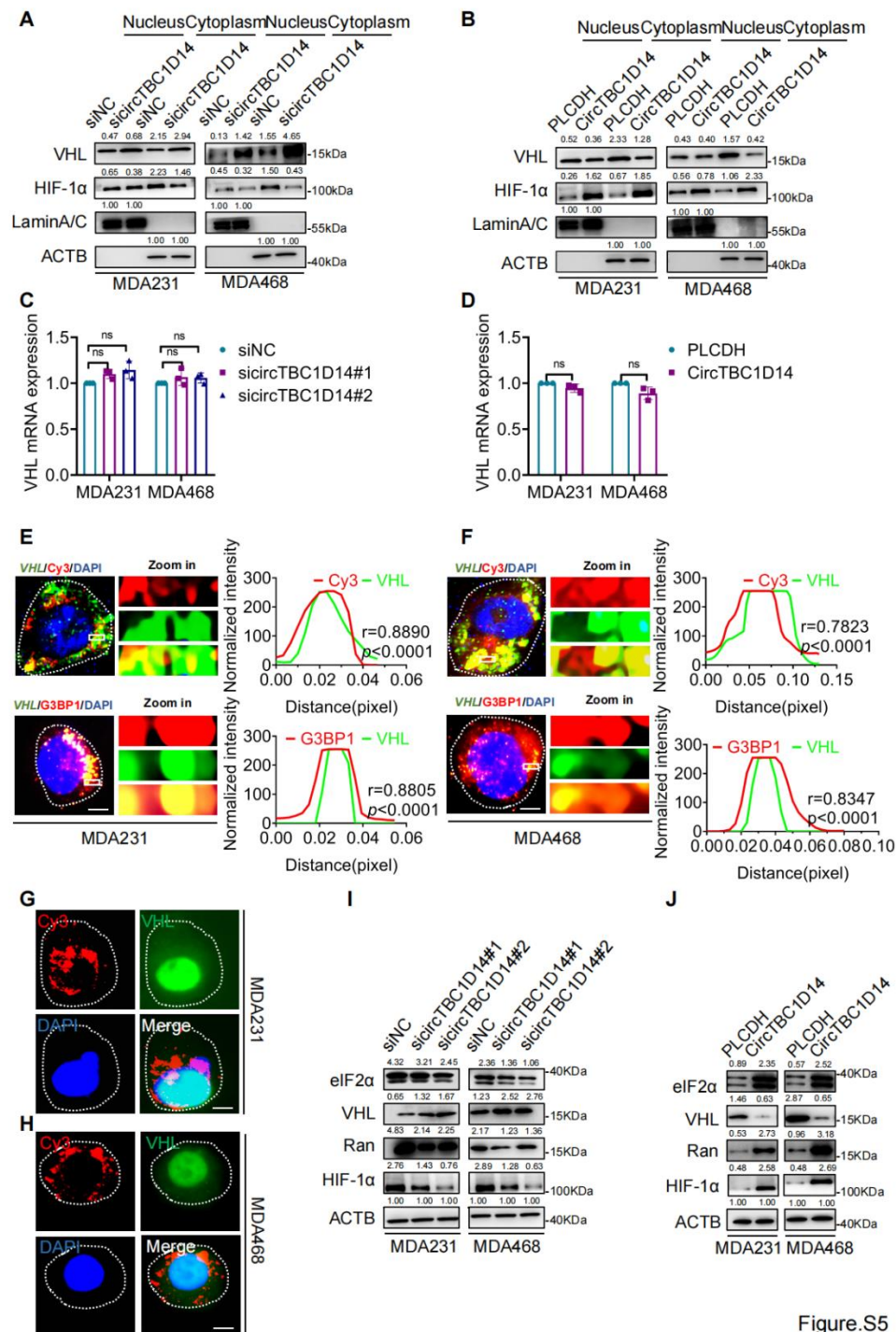


Figure.S5

**Figure. S5 CircTBC1D14 stabilized hypoxia-inducible factor-1-alpha (HIF-1α) expression by inhibiting the translation of von Hippel-Lindau (VHL).** A and B) Western blot analysis of relative distribution with circTBC1D14 overexpression or knockdown in MDA231 and MDA468 cells. C and D) Quantitative real-time PCR analysis of VHL expression in MDA231 or MDA468

cells with circTBC1D14 overexpression or knockdown condition. Two-tailed unpaired t-test. E and F) RNA FISH of VHL and circTBC1D14 or SGs (G3BP1+) in MDA231 and MDA468 cells. Scale bar, 10  $\mu$ m. Right, Pearson correlation analysis of VHL and circTBC1D14 or SGs (G3BP1+) co-localizing. G and H) FISH of circTBC1D14 and VHL protein in MDA231 and MDA468 cells. Scale bar, 10  $\mu$ m. I and J) Western blot analysis of relative expression with circTBC1D14 overexpression or knockdown in MDA231 and MDA468 cells. The data are shown as the mean  $\pm$ SD, NS (no significance) \* $P$  < 0.05 \*\* $P$  < 0.01, \*\*\* $P$  < 0.001.

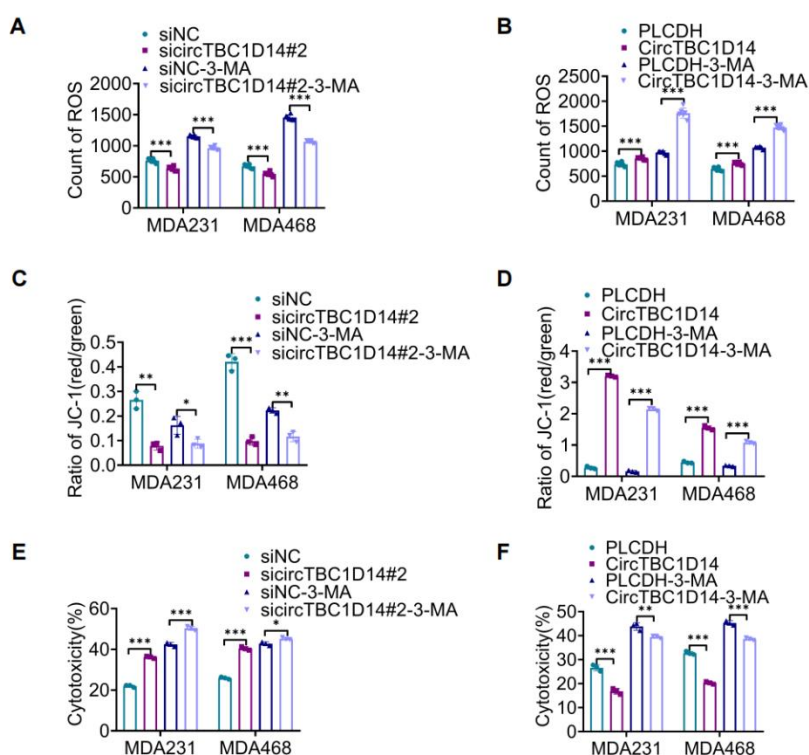


Figure. S6

**Figure. S6 CircTBC1D14 regulated cell death via autophagy in hypoxic conditions.** A and B) Quantification of the count of ROS with circTBC1D14 overexpression or knockdown in MDA231 and MDA468 cells after 3-MA (5mM) and hypoxia treatment. Two-tailed unpaired t-test. C and D) Quantification of the ratio of JC-1 with circTBC1D14 overexpression or knockdown in MDA231 and MDA468 cells after 3-MA (5mM) and hypoxia treatment. Two-tailed unpaired t-test. E and F) Quantification of the percentage of cytotoxicity with circTBC1D14 overexpression or knockdown in MDA231 and MDA468 cells after 3-MA (5mM) and hypoxia treatment. Two-tailed unpaired



t-test. The data are shown as the mean  $\pm$ SD, NS (no significance) \*P < 0.05 \*\*P < 0.01, \*\*\*P < 0.001.

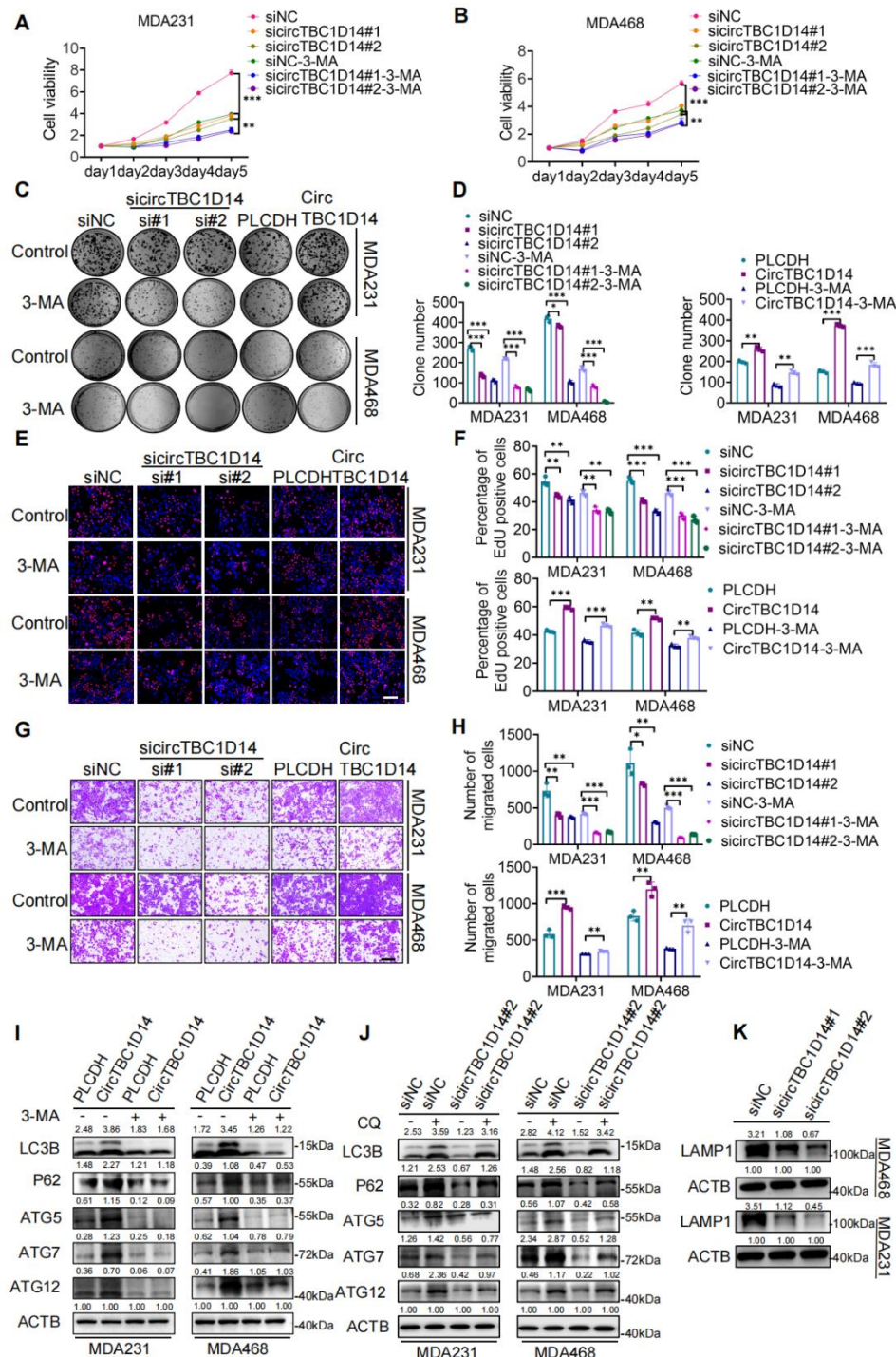


Figure.S7

**Figure. S7 CircTBC1D14 promoted TNBC proliferation and metastasis through autophagy.**

A and B) Cell viability of MDA231 and MDA468 cells with circTBC1D14 overexpression or

knockdown compared to control cells after 3-MA (5mM) treatment. Two-tailed unpaired t-test. C) Clone formation of MDA231 and MDA468 cells with circTBC1D14 overexpression or knockdown compared to control cells after 3-MA (5mM) treatment. D) Statistical diagram of C). Two-tailed unpaired t-test. E) EdU assay of MDA231 and MDA468 cells with circTBC1D14 overexpression or knockdown compared to control cells after 3-MA (5mM) treatment. Scale bar, 20  $\mu$ m. F) Statistical diagram of E). Two-tailed unpaired t-test. G) Transwell assay of MDA231 and MDA468 cells with circTBC1D14 overexpression or knockdown compared to control cells after 3-MA (5mM) treatment. Scale bar, 20  $\mu$ m. H) Statistical diagram of G). Two-tailed unpaired t-test. I) Western blot analysis of relative expression with circTBC1D14 overexpression after 3-MA (5mM) treatment or not in MDA231 and MDA468 cells. J) Western blot analysis of relative expression with circTBC1D14 knockdown after CQ (25  $\mu$ M) treatment or not in MDA231 and MDA468 cells. K) Western blot analysis of relative expression with circTBC1D14 knockdown in MDA231 and MDA468 cells. The data are shown as the mean  $\pm$ SD, NS (no significance) \* $P$  < 0.05 \*\* $P$  < 0.01, \*\*\* $P$  < 0.001.

## Supplementary Tables

**Table S1 Sequences of siRNA used in this study**

| Definition      | sequences                    |
|-----------------|------------------------------|
| siCircTBC1D14#1 | 5'-UAAAUUAUCACCCACGUUUCTT-3' |
| siCircTBC1D14#2 | 5'-CACCCACGUUUCUCCUUGGTT-3'  |
| siNC            | 5'-UUCUCCGAACGUGUCACGUTT-3'  |
| siFUS#1         | 5'-CAGAGUUACAGUGGUUAUA-3'    |
| siFUS#2         | 5'-CCAAUUCCUGAUCACCCAA-3'    |
| siPRMT1#1       | 5'-GCGAGGAGATCTTCGGCACCA-3'  |
| siPRMT1#2       | 5'-GGACATGACATCCAAAGAT-3'    |
| siLAMP1         | 5'-AGAAAUGCAACACGUUAUU-3'    |

**Table S2 Sequences of primer used in this study**

| Gene          | Primer sequences   |
|---------------|--|
| GAPDH         | F: 5'-GTCTCCTCTGACTTCAACAGCG-3'<br>R: 5'-ACCACCCTGTTGCTGTAGCCAA-3' |
| U6            | F: 5'-CTCGCTTCGGCAGCACAT-3'<br>R: 5'-TTTGCGTGTTCATCCTTGCG-3'       |
| CircTBC1D14   | F: 5'-GCTTAGCCATTGGCAACGAG-3'<br>R: 5'-GAAGGGGGTTTCCTGGTCG-3'      |
| LinearTBC1D14 | F: 5'-GACCAGGAAACCCCTTCAG-3'<br>R: 5'-AGGGTAGGAATCCCGAGTC-3'       |
| ATCB          | F: 5'-CACCATTGGCAATGAGCGGTTC-3'<br>R: 5'-AGGTCTTTGCGGATGTCCACGT-3' |
| FUS           | F: 5'-CAAGGCCTGGGTGAGAATGT-3'<br>R: 5'-TTGCCTCTCCCTTCAGCTTG-3'     |
| TBC1D14       | F: 5'-GAAACGCTGTGCTCACCTGGAA-3'<br>R: 5'-GCTCCAGACTTTGCCTCTCACA-3' |
| PRMT1         | F: 5'-TGCGGTGAAGATCGTCAAAGCC-3'<br>R: 5'-GGACTCGTAGAAGAGGCAGTAG-3' |
| LAMP1         | F: 5'-CGTGTACGAAGGCGTTTTTCAG-3'<br>R: 5'-CTGTTCTCGTCCAGCAGACACT-3' |

**Table S3 List of antibodies used in this study**

| <b>Antibody</b>   | <b>Catalog Number</b> | <b>Company</b>                         |
|---|-----------------------|--|
| Anti-human ATG5 Rabbit Polyclonal Antibody  | 10181-2-AP            | Proteintech Group, Inc                 |
| Anti-human ATG7 Rabbit Polyclonal Antibody  | 10088-2-AP            | Proteintech Group, Inc                 |
| Anti-human ATG12 Rabbit Polyclonal Antibody   | 11122-1-AP            | Proteintech Group, Inc                 |
| Anti-human LC3 Rabbit Polyclonal Antibody   | 14600-1-AP            | Proteintech Group, Inc                 |
| Anti-human GAPDH Rabbit Polyclonal Antibody   | 10494-1-AP            | Proteintech Group, Inc                 |
| Anti-human Lamin A/C Rabbit Polyclonal Antibody                                       | 10298-1-AP            | Proteintech Group, Inc                 |
| Anti-human Beta Actin Mouse Monoclonal Antibody                                       | 66009-1-Ig            | Proteintech Group, Inc                 |
| Anti-human MYC-Tag Mouse Monoclonal antibody  | 60003-2-Ig            | Proteintech Group, Inc                 |
| Anti-human Flag-Tag Rabbit Polyclonal antibody  | 20543-1-AP            | Proteintech Group, Inc                 |
| Anti-human HA-Tag Mouse Monoclonal Antibody   | 66006-2-Ig            | Proteintech Group, Inc                 |
| Anti-human FUS Rabbit Polyclonal Antibody   | 11570-1-AP            | Proteintech Group, Inc                 |
| Anti-human PRMT1 Rabbit Polyclonal Antibody   | 11279-1-AP            | Proteintech Group, Inc                 |
| Anti-human LAMP1 Rabbit Polyclonal Antibody   | 21997-1-AP            | Proteintech Group, Inc                 |
| Anti-human KI67 Rabbit Polyclonal antibody  | 27309-1-AP            | Proteintech Group, Inc                 |
| Anti-human G3BP1 Rabbit Polyclonal antibody   | 13057-2-AP            | Proteintech Group, Inc                 |
| Anti-human P62 Mouse Monoclonal Antibody  | sc-28359              | Santa Cruz Biotechnology               |
| Anti-human VHL Mouse Monoclonal Antibody  | sc-135657             | Santa Cruz Biotechnology               |
| Anti-human Ran Mouse Monoclonal Antibody  | sc-271376             | Santa Cruz Biotechnology               |
| Anti-human eIF4AIII Mouse Monoclonal Antibody   | sc-365549             | Santa Cruz Biotechnology               |
| Anti-human PARP1 Mouse Monoclonal antibody  | sc-8007               | Santa Cruz Biotechnology               |
| Anti-human FMRP Rabbit Monoclonal Antibody  | 4317                  | Cell Signaling Technology              |
| Anti-human HIF-1 $\alpha$ Rabbit Monoclonal Antibody                                  | 36169                 | Cell Signaling Technology              |
| Goat anti-Rabbit IgG (H+L) Highly Cross-Adsorbed Secondary Antibody, Alexa Fluor® 488 | ZF-0511               | Zhong Shan Golden Bridge Biotechnology |
| Goat anti-Rabbit IgG (H+L) Cross-Adsorbed Secondary Antibody, TRITC                   | ZF-0317               | Zhong Shan Golden Bridge Biotechnology |
| Goat anti-Mouse IgG (H+L) Highly Cross-Adsorbed Secondary Antibody, Alexa Fluor® 488  | ZF-0513               | Zhong Shan Golden Bridge Biotechnology |